

## Surface Energy and Thermodynamic Stability of $\gamma$ -Alumina: Effect of Dopants and Water

Ricardo H. R. Castro,<sup>†,‡</sup> Sergey V. Ushakov,<sup>‡</sup> Leon Gengembre,<sup>§</sup> Douglas Gouvêa,<sup>⊥</sup> and Alexandra Navrotsky<sup>\*,‡</sup>

Centro Universitário da FEI, Av. Humberto A.C. Branco 3973, São Bernardo do Campo SP 09850-901, Brazil, Thermochemistry Facility and NEAT ORU, University of California, Davis, 1 Shields Avenue, Davis, California 95616, Laboratoire de Catalyse de Lille – École Nationale Supérieure de Chimie de Lille, France, and Department of Metallurgical and Materials Engineering, University of São Paulo, Av. Prof. Mello Moraes 2463, Cidade Universitária, São Paulo SP 05353-080, Brazil

Received November 24, 2005. Revised Manuscript Received January 31, 2006

Retaining large surface areas in alumina powders during high-temperature annealing is a major challenge in applications as catalyst supports and ceramic precursors. This is because the alumina surface area drastically decreases with transformation from the  $\gamma$  modification (defect spinel structure) into the  $\alpha$  modification (corundum structure). The objective of this work is to show the thermodynamic basis of using additives, such as Zr and Mg, to control the  $\gamma$ -Al<sub>2</sub>O<sub>3</sub> surface and bulk energetics and to manipulate the transformation temperature and surface area. These additives are observed to change the pattern of phase transformation and densification. Direct measurements of heats of solution in a lead borate melt of pure and doped alumina as a function of surface area enabled us to experimentally derive trends in the surface energies of hydroxylated surfaces. Accounting for heats of water adsorption measured on pure and doped alumina surfaces allowed us to delineate the thermodynamic effects of hydration on surface energies. Zr-doped  $\gamma$ -alumina showed a higher energy of the hydroxylated surface than did pure  $\gamma$ -alumina but showed a lower energy of the anhydrous surface. Mg addition does not change surface energies significantly but decreases the energetic instability of the bulk  $\gamma$  phase.

### Introduction

The fabrication of functional catalysts, ceramics, thin films, and nanostructures is, to a large extent, a manipulation of surface and interfacial energies. Thermodynamically, the combination of surface and bulk energies defines which polymorph is the most stable at a given surface area and provides a driving force for coarsening, size-induced transformations, and compositional changes in the interfaces. Recent works document competition between the energetics of polymorphism and surface energies in several oxide systems,<sup>1–3</sup> resulting in free energy crossovers at the nano-scale level. Kinetically, surface/interface energies together with diffusion parameters define the energetic barriers for nucleation and pathways of phase transformation.

The rapidly growing field of theoretical calculations and simulations of energies of surfaces and interfaces in oxides, despite being an important tool for predicting structure and morphology, begs for experimental benchmarks. Solution

calorimetry allows for the measurement of surface enthalpies by measuring the heat evolved on the dissolution of a material with varying surface area in a suitable solvent. The first application of high-temperature oxide melt solution calorimetry for measuring surface energies<sup>3,4</sup> established that  $\gamma$ -alumina is thermodynamically stabilized over corundum ( $\alpha$ -Al<sub>2</sub>O<sub>3</sub>) at room temperature by the surface term at surface areas greater than about 125 m<sup>2</sup> g<sup>-1</sup>. But the question remains of how to control the surface energies to achieve a desired microstructure development. In the present study, we apply high-temperature oxide melt solution calorimetry and water adsorption microcalorimetry to delineate the effect of Zr and Mg additives on surface energies of  $\gamma$ -alumina and evaluate the consequences for the phase transformation and microstructure evolutions. Effects of these typical dopants were previously discussed<sup>5–7</sup> exclusively on kinetic grounds; the effect of these additives of raising the transformation temperature is attributed to their ability to hamper diffusion in  $\gamma$ -Al<sub>2</sub>O<sub>3</sub>.

### Experimental Section

**Synthesis.** Powders were prepared by the polymeric precursor method, also known as a derivative of Pechini's method.<sup>8–11</sup> Al-

\* To whom correspondence should be addressed. E-mail: anavrotsky@ucdavis.edu. Fax: (530) 752-9307. Tel.: (530) 752-3292.

<sup>†</sup> Centro Universitário da FEI.

<sup>‡</sup> University of California, Davis.

<sup>§</sup> École Nationale Supérieure de Chimie de Lille.

<sup>⊥</sup> University of São Paulo.

- (1) Pitcher, M. W.; Ushakov, S. V.; Navrotsky, A.; Woodfield, B. F.; Li, G. S.; Boerio-Goates, J.; Tissue, B. M. *J. Am. Ceram. Soc.* **2005**, *88*, 160.
- (2) Navrotsky, A. *Abstracts of Papers*, 225th National Meeting of the American Chemical Society, New Orleans, LA, March 23–27, 2003, American Chemical Society: Washington, DC, 2003; U939.
- (3) McHale, J. M.; Auroux, A.; Perrotta, A. J.; Navrotsky, A. *Science* **1997**, *277*, 788.

- (4) McHale, J. M.; Navrotsky, A.; Perrotta, A. J. *J. Phys. Chem. B* **1997**, *101*, 603.

- (5) Okada, K.; Hattori, A.; Taniguchi, T.; Nukui, A.; Das, R. N. *J. Am. Ceram. Soc.* **2000**, *83*, 928.

- (6) Xue, L. A.; Chen, I. W. *J. Mater. Sci. Lett.* **1992**, *11*, 443.

- (7) Djuricic, B.; Pickering, S.; Glaude, P.; McGarry, D.; Tambuyser, P. *J. Mater. Sci.* **1997**, *32*, 589.

(NO<sub>3</sub>)<sub>3</sub>·9H<sub>2</sub>O (Alfa Aesar, 99.8%) was used as the aluminum precursor, magnesium nitrate (Alfa Aesar, 99.95%) as the magnesium precursor, and zirconium carbonate (Alfa Aesar, 99.9%) as the zirconium source. A solution containing 25 wt % aluminum nitrate, 30 wt % ethylene glycol, and 45 wt % citric acid was prepared and mixed until all components dissolved at 70 °C. Thereafter, the solution was heated to 120 °C for polyesterification for 15 min. Carbonate salts of Mg and Zr were dissolved in 30 vol % HNO<sub>3</sub> and added to the obtained liquid resin. Amounts of additives were calculated to achieve 3 and 5 mol % MgO and 1 and 2 mol % ZrO<sub>2</sub>. The resins were treated at 450 °C for 4 h, and the resulting carbon-rich powder was ground in an alumina mortar. The ground powders were then treated at 650 °C for 15 h in air to burn most of remaining organic material. After thermal analysis, samples were heated at 10 °C/min and quenched in air from temperatures selected to obtain  $\gamma$ -Al<sub>2</sub>O<sub>3</sub> with varying specific surface areas ( $S_{\text{BET}}$ ). For solution calorimetry measurements, these temperatures were never lower than 950 °C in order to avoid carbon contamination.

**Electron Probe Microanalysis and X-ray Photoelectron Spectroscopy (XPS).** Zr and Mg concentrations in synthesized samples were measured by wavelength dispersive (WD) electron probe microanalysis using a Cameca SX100 microprobe at accelerating voltage 15 kV, 10 nA beam current, and 5  $\mu\text{m}$  beam size. Analytic lines and crystals were Al K $\alpha$  and Mg K $\alpha$  on TAP, and Zr L $\alpha$  on PET. For analysis, powders were pelletized, sintered at 1500 °C, polished, and carbon-coated. XPS measurements were carried out on Zr-doped  $\gamma$ -Al<sub>2</sub>O<sub>3</sub> powders pressed into thin pellets on In foils. A VG ESCALAB 220XL spectrophotometer was used at a pressure  $<10^{-7}$  Pa with Al K $\alpha$  (1486.6 eV) nonmonochromatized radiation for excitation and an analyzer pass energy of 40 eV. The 2p level with energy  $74.6 \pm 0.2$  eV was used to detect Al atoms, 3d<sup>5</sup> with energy  $182.9 \pm 0.2$  eV was used to detect Zr, and standard C<sub>1s</sub> was determined at  $285.15 \pm 0.2$  eV. Elemental ratios were obtained using Eclipse (ThermoVG Scientific) software.

**Powder X-ray Diffraction (XRD).** Powder X-ray diffraction (XRD) was used to characterize phase transformation in pure and doped alumina. An INEL-CPS120 diffractometer was operated at 30 kV and 30 mA (Cu K $\alpha$  radiation, incident beam monochromator). High-temperature measurements were performed in air with a heating rate of 5 °C min<sup>-1</sup> and dwell time of 1 h. All as-prepared powders (650 °C for 15 h to anneal) were amorphous from XRD. An amorphous- $\gamma$ - $\alpha$  sequence was observed on heating of doped samples and no transitional aluminas were observed on heating or cooling.

**Thermal Analysis (DSC).** Differential scanning calorimetry (DSC) and thermogravimetry (TG) measurements were carried out using a Netzsch STA 449 system. Samples were heated at 10 °C min<sup>-1</sup> from room temperature to 1400 °C under an air flow (40 mL min<sup>-1</sup>). Sensitivity was calibrated by the Cp method with a sapphire standard. Uncertainties in derived enthalpies of phase transformation were estimated as  $\pm 5\%$ .

**Surface Area Measurements and Water Adsorption Microcalorimetry.** Specific surface areas were measured by N<sub>2</sub> adsorption using a 5-point Brunauer–Emmett–Teller (BET) technique with a surface-area analyzer (ASAP 2020 Micromeritics, Norcross, GA) equipped with turbo pumps on the degas and analysis side. Prior to measurements being made, samples were degassed in vacuo at

**Table 1. High-Temperature Solution and Water Adsorption Calorimetry Data for Pure and Doped  $\gamma$ -Al<sub>2</sub>O<sub>3</sub>**

sample	$T_{\text{synth}}$ (°C)	$S_{\text{BET}}$ (m <sup>2</sup> /g)	H <sub>2</sub> O <sup>a</sup> (wt %)	$\Delta H_{\text{ds}}^b$ (J/g)	$\Delta H_{\text{des}}^c$ (J/g)	
Al <sub>2</sub> O <sub>3</sub>	950	132.6	10.25	1037 $\pm$ 20(9)	188	
	985	105.5	8.85	982 $\pm$ 9 (4)	150	
	1005	89.9	9.70	1004 $\pm$ 20(8)	127	
	1010	89.0	8.03	978 $\pm$ 14(6)	126	
	1015	78.1	7.62	983 $\pm$ 11(7)	111	
	1020	73.8	6.59	958 $\pm$ 12(8)	105	
	1025	72.8	7.02	964 $\pm$ 23(7)	103	
	3% Mg	1040	102.5	8.96	1012 $\pm$ 17(8)	169
		1060	94.1	6.72	1017 $\pm$ 15(6)	155
	5% Mg	950	147.6	11.66	1123 $\pm$ 10(4)	243
1040		100.3	7.76	1003 $\pm$ 16(6)	165	
1050		95.7	6.93	979 $\pm$ 23(12)	158	
1060		93.6	8.66	1005 $\pm$ 8(8)	154	
1065		91.8	7.74	994 $\pm$ 13(8)	151	
1% Zr	1075	76.2	5.75	976 $\pm$ 8(9)	126	
	1000	25.8	3.74	867 $\pm$ 11(7)	7	
	1155	17.2	3.24	884 $\pm$ 24(6)	5	
	1175	13.7	3.56	859 $\pm$ 32 (6)	4	
2% Zr	1190	9.4	1.37	830 $\pm$ 28 (4)	3	
	1000	29.4	2.62	814 $\pm$ 15 (3)	8	
	1190	11.3	3.93	853 $\pm$ 10 (5)	3	

<sup>a</sup> Measured after equilibration at 45% humidity prior to solution calorimetry. <sup>b</sup> Errors are two standard deviations of the mean; the number of experiments is given in parentheses. <sup>c</sup> For the reaction  $\text{Al}_2\text{O}_3 \cdot x\text{H}_2\text{O}_{(s,25^\circ\text{C})} = \text{Al}_2\text{O}_3_{(s,25^\circ\text{C})} + x\text{H}_2\text{O}_{(l,25^\circ\text{C})}$  from adsorption microcalorimetry experiments.

450 °C for 2 h. For water adsorption microcalorimetry experiments, a surface-area analyzer was used in combination with a Calvet-type microcalorimeter<sup>12</sup> (Setaram DSC-111). Samples were quenched in air from 1000 °C. Samples (50–150 mg) were placed in one side of a quartz fork-type tube ( $\sim 10$  cm<sup>3</sup>), and the total surface area of the sample and free volume of the tube were measured after degassing at 750 °C for 2 h. The residual volatiles left in the sample were measured as the difference between weight losses on heating to 1550 °C for 12 h and on degassing. The dosing routine provided an adsorbed amount of  $\sim 2$   $\mu\text{mol}$  H<sub>2</sub>O per dose and an equilibration time of  $\sim 1$  h. For the calculation of differential heats of water adsorption, we made a correction for water adsorption on the tube and manifold from a blank run in the same conditions. The preadsorbed coverage varied for each sample and was determined to be 2.86 OH nm<sup>-2</sup> for the pure  $\gamma$ -Al<sub>2</sub>O<sub>3</sub>, 1.99 OH nm<sup>-2</sup> for Mg-doped  $\gamma$ -Al<sub>2</sub>O<sub>3</sub>, and 3.31 OH nm<sup>-2</sup> for the Zr-doped sample. The adsorption enthalpies for preadsorbed amounts were determined by linearly extrapolating the integral heats of adsorption, forcing an intercept at the origin.

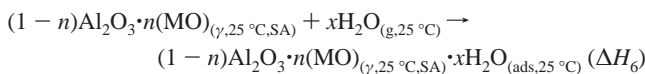
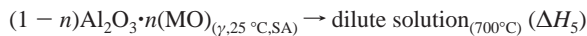
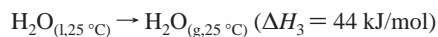
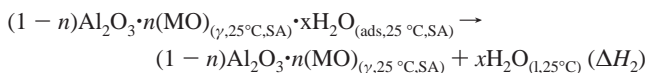
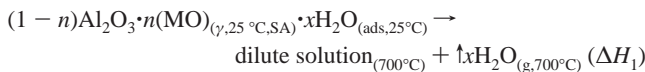
**High-Temperature Oxide Melt Solution Calorimetry.** High-temperature oxide melt drop solution calorimetry was performed in a custom-made isoperibol Tian-Calvet twin microcalorimeter.<sup>13</sup> Samples were pressed into  $\sim 5$  mg pellets, weighed, and dropped from room temperature into 2PbO·B<sub>2</sub>O<sub>3</sub> solvent at 702 °C. Water vapor, evolved from solvent on dissolution, was flushed out of the calorimeter with an oxygen flow (40 mL min<sup>-1</sup>), providing a return to the initial baseline.<sup>14</sup> The calorimeter was calibrated against the heat content of  $\alpha$ -Al<sub>2</sub>O<sub>3</sub> pellets of similar volume. Prior to performing calorimetric experiments, we exposed pure and doped  $\gamma$ -Al<sub>2</sub>O<sub>3</sub> samples for several days to 45% relative humidity at 25 °C. Equilibrium water contents were determined from weight loss after transformation to coarse corundum by annealing in air at 1550 °C for 12 h.

(8) Pechini, M.; U.S. Patent 3 330 697, July 11, 1967.  
 (9) Gouvea, D.; Villalobos, R. L.; Capocchi, J. D. T. *Mater. Sci. Forum* **1999**, *299*, 91.  
 (10) Lessing, P. A. *Am. Ceram. Soc. Bull.* **1989**, *68*, 1002.  
 (11) Bernardi, M. I. B.; Crispim, S. C. L.; Maciel, A. P.; Souza, A. G.; Conceicao, M. M.; Leite, E. R.; Longo, E. J. *J. Therm. Anal. Calorim.* **2004**, *75*, 475.

(12) Ushakov, S. V.; Navrotsky, A. *Appl. Phys. Lett.* **2005**, *87*, 164103.  
 (13) Navrotsky, A. *Phys. Chem. Miner.* **1977**, *2*, 89.  
 (14) Navrotsky, A.; Rapp, R. P.; Smelik, E.; Burnley, P.; Circone, S.; Chai, L.; Bose, K. *Am. Mineral.* **1994**, *79*, 1099.

**Calculation of Surface Enthalpies from Solution and Adsorption Calorimetry Data.** Table 1 summarizes experimental data. Drop solution experiments were performed on samples kept at 45% relative humidity at 25 °C, and equilibrium water content was calculated from weight loss after prolonged annealing at 1450 °C, causing transformation to coarse  $\alpha$ -alumina. In previous high-temperature oxide melt solution calorimetry experiments,<sup>14</sup> it was shown that water is not retained in the lead borate solvent but evolves as vapor. To derive surface energies of hydroxylated surfaces, we took the reference state of water adsorbed on the surface as liquid water. To derive surface energies of anhydrous surfaces, we measured water adsorption enthalpies and accounted for them in thermochemical cycles. Because the  $P\Delta V$  terms are small for solid and liquid phases, the energy ( $\Delta E$ ) and enthalpy ( $\Delta H$ ) are essentially identical, and the terms surface energy and surface enthalpy can be used interchangeably. Note also that although dissolution takes place at high temperature, the surface enthalpy obtained is at room temperature.

In the thermochemical cycle shown below,  $n$  stands for concentration of dopant in  $\gamma$ - $\text{Al}_2\text{O}_3$  SA is the surface area of the sample and  $x$  is equilibrium water content adsorbed before calorimetry (Table 1)



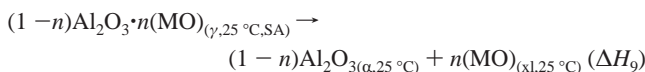
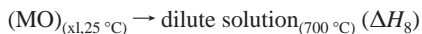
$$\Delta H_5 = \Delta H_1 - \Delta H_2 - x\Delta H_3 - x\Delta H_4$$

“Hydroxylated surfaces”  $\Delta H_2 = 0$  and  $\Delta H_5 =$

$$\Delta H_1 - x(\Delta H_3 + \Delta H_4)$$

“Anhydrous surfaces”  $\Delta H_2 = -\Delta H_6 - x\Delta H_3$  and  $\Delta H_5 =$

$$\Delta H_1 + \Delta H_6 - x\Delta H_4$$



$$\Delta H_9 = \Delta H_5 - (1-n)\Delta H_7 - n\Delta H_8$$

where  $\Delta H_1$  is the measured enthalpy of the drop solution,  $\Delta H_6$  is the integral of the measured differential enthalpies of adsorption for a given  $x$ , and  $\Delta H_9$  is the enthalpy with respect to coarse  $\alpha$ - $\text{Al}_2\text{O}_3$  ( $\Delta H$  wrt coarse  $\alpha$ - $\text{Al}_2\text{O}_3$  in Figure 4).  $\Delta H_3$ ,  $\Delta H_4$ , and  $\Delta H_7$  are reference values.<sup>15</sup> MO stands for  $\text{ZrO}_2$  and  $\text{MgO}$  in doped samples and  $\Delta H_8 = \Delta H_{\text{ds}}(\text{ZrO}_2) = 70.1 \text{ kJ/mol}^1$  for Zr-doped samples and  $\Delta H_8 = \Delta H_{\text{ds}}(\text{MgO}) = 31.7 \text{ kJ/mol}^{16,17}$  for Mg-doped

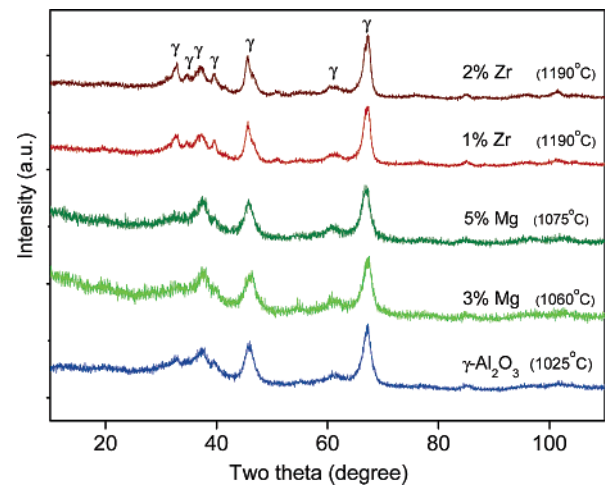


**Figure 1.** XRD patterns for pure and doped  $\text{Al}_2\text{O}_3$  samples (Cu K $\alpha$  radiation). Samples were quenched from the temperatures given in parentheses.  $\gamma$ - $\text{Al}_2\text{O}_3$  reflection markers are given after ref 18.

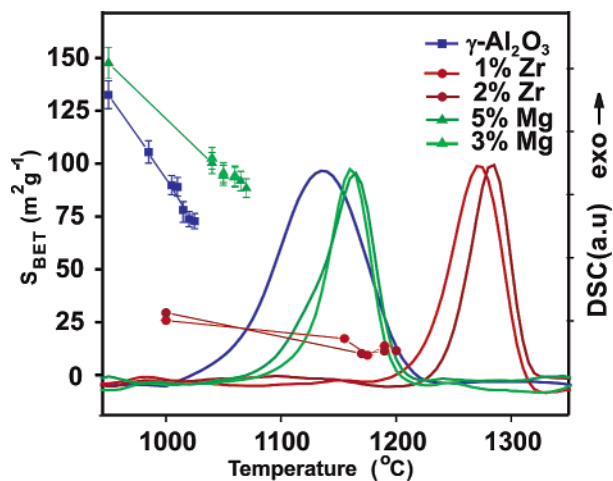


**Figure 2.** Portions of DSC traces for pure and doped  $\text{Al}_2\text{O}_3$  samples showing exothermic peaks corresponding to the  $\gamma$ - $\alpha$  transition. The points depict the specific surface areas ( $S_{\text{BET}}$ ) of  $\gamma$ - $\text{Al}_2\text{O}_3$  used for calorimetric experiments and the temperatures they were quenched from.

samples. All weight losses of the samples used for calorimetry were assumed to be due to water adsorbed on the surface. The values of the drop solution enthalpies are specific for the solvent used. The values of excess enthalpy with respect to coarse corundum are independent of solvent used and depend only on differences in surface and bulk energies.

## Results and Discussion

Series of pure and doped  $\gamma$ -alumina samples with different surface areas were prepared by calcination of polymeric precursors at different temperatures below the transformation to  $\alpha$ -alumina. Figure 1 shows XRD patterns of the samples in which only the  $\gamma$ - $\text{Al}_2\text{O}_3$  spinel structure can be observed.<sup>18</sup> Figure 2 shows surface areas for the samples used for calorimetry and the exotherms in differential scanning calorimetry (DSC) traces for the  $\gamma$ -to- $\alpha$  transformation for each studied composition (see Experimental Section for details). The enthalpies of transformation become less exothermic with increasing dopant concentration:  $-19.4 \text{ kJ}$

(15) Putnam, R. L.; Navrotsky, A.; Cordfunke, E. H. P.; Huntelaar, M. E. *J. Chem. Thermodyn.* **2000**, *32*, 911.

(16) Davies, P. K.; Navrotsky, A. *J. Solid State Chem.* **1981**, *38*, 264.

(17) Davies, P. K.; Navrotsky, A. In *Proceedings of Symposium on High-Temperature Materials Chemistry*, Cubicciotti, D. B., Hildenbrand, D. L., Eds.; The Electrochemical Society: Pennington, NJ, 1982; 118.

(18) Youn, H. J.; Jang, J. W.; Kim, I. T.; Hong, K. S. *J. Colloid Interface Sci.* **1999**, *211*, 110.

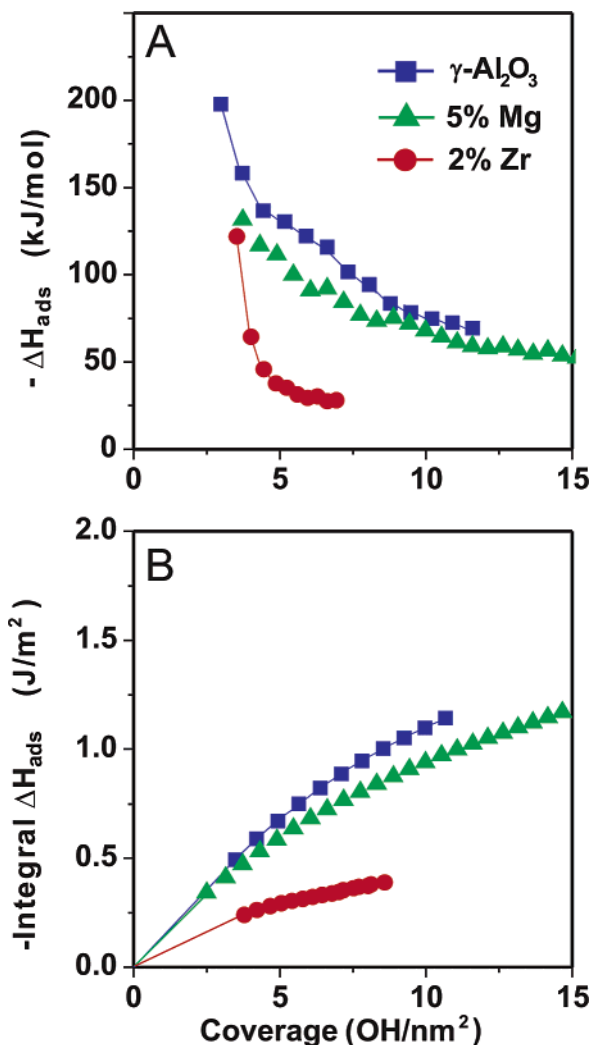


**Figure 3.** Differential (A) and integral (B) heats of H<sub>2</sub>O adsorption on pure and doped  $\gamma$ -Al<sub>2</sub>O<sub>3</sub> as a function of hydroxyl coverage.

mol<sup>-1</sup> for pure Al<sub>2</sub>O<sub>3</sub>; -13.2 and -12.7 kJ per mole of Al<sub>2</sub>O<sub>3</sub> for alumina with 1 and 2 mol % ZrO<sub>2</sub>; -17.8 and -16.7 kJ per mole for samples with 3 and 5 mol % MgO. Both additives increase the temperature for onset of the  $\gamma$ -to- $\alpha$  transformation: from 1025 °C for pure  $\gamma$ -Al<sub>2</sub>O<sub>3</sub> to 1075–1077 °C for Mg-doped and 1190–1195 °C for Zr-doped samples. For Mg-doped samples, the surface area before transformation to  $\alpha$ -Al<sub>2</sub>O<sub>3</sub> is similar to that for pure  $\gamma$ -alumina ( $\sim 75$  m<sup>2</sup> g<sup>-1</sup>), whereas for Zr-doped samples, it decreases to  $\sim 10$  m<sup>2</sup> g<sup>-1</sup> before transformation. Notably, although Zr-doped samples show the most significant increase in transformation temperature compared with pure alumina, the specific surface area of the powders before transformation is much lower for Zr-doped samples than for pure and Mg-doped alumina, and this area decreases with temperature much less rapidly than it does for pure and Mg-doped materials. Calorimetric data reported below provide thermodynamic insight into this observation.

Figure 3 shows the adsorption microcalorimetry experiments presented as a function of hydroxyl coverage, assuming that one molecule of water generates two OH groups on the surface. This scale was chosen to be consistent with reports of dissociative behavior of H<sub>2</sub>O adsorption on alumina surfaces at these coverages.<sup>19–21</sup> However, because we

directly measure heat of adsorption in our experiments, assumptions with respect to speciation of water on the surface do not affect the derivation of surface energies.

The differential heats of H<sub>2</sub>O adsorption on all samples show regular logarithmic decay with surface coverage, which is consistent with previous work on alumina.<sup>3,20,22</sup> Adsorption enthalpies for pure  $\gamma$ -alumina agree with those previously reported.<sup>3,20,22</sup> The correction for the adsorbed water for 5 OH nm<sup>-2</sup> coverage is -130 kJ mol<sup>-1</sup> H<sub>2</sub>O (liquid) for pure  $\gamma$ -Al<sub>2</sub>O<sub>3</sub>, -110 kJ mol<sup>-1</sup> for Mg-doped  $\gamma$ -Al<sub>2</sub>O<sub>3</sub>, and only -38 kJ mol<sup>-1</sup> for the Zr-doped sample. Such a decrease in the magnitude of the enthalpy of adsorption for the Zr-doped sample is a strong indication of a lowering of surface energy of  $\gamma$ -alumina by this additive, because the heat of chemisorption of H<sub>2</sub>O is expected to be directly proportional to the surface energy of the anhydrous phase, as previously reported by McHale et al.<sup>3</sup> and predicted by Cerofolini.<sup>23</sup> To quantify surface enthalpies, one must analyze the solution calorimetry results.

The enthalpies of drop solution for hydrous samples of pure and doped  $\gamma$ -alumina are summarized in Table 1 together with water contents of the samples. In Figure 4, the excess enthalpies for hydroxylated and anhydrous pure and doped  $\gamma$ -alumina are fitted with linear trends as functions of surface area ( $\Delta H_{\text{wrt } \alpha\text{-Al}_2\text{O}_3} = H_0 + H_{\text{surf}}SA$ ). For a given composition and structure, the slope ( $H_{\text{surf}}$ ) corresponds to average surface enthalpy. The intercept at zero surface area ( $H_0$ ) represents bulk stability with respect to the chosen alumina reference state, coarse corundum and the additives cubic MgO and monoclinic ZrO<sub>2</sub>. Surface enthalpies for doped and pure  $\gamma$ -Al<sub>2</sub>O<sub>3</sub> are listed in Table 2 together with reference data.<sup>24</sup> Variations of enthalpies in samples doped with 1 and 2% Zr and in samples doped with 3 and 5% Mg were found to be within experimental uncertainties (Figure 4), so all data for each dopant were used for linear fit.

From Figure 4, excess enthalpy values at zero surface area indicate that pure and Zr-doped  $\gamma$ -alumina are  $29 \pm 2$  kJ/mol and  $28 \pm 3$  kJ/mol, respectively, less stable than the coarse  $\alpha$ -alumina phase +  $m$ -ZrO<sub>2</sub>. The excess enthalpy value for  $\gamma$ -Al<sub>2</sub>O<sub>3</sub> doped with Mg is  $24 \pm 3$  kJ/mol above that for coarse Al<sub>2</sub>O<sub>3</sub> + MgO, showing a slight gain in stability. The slopes of the trends for hydroxylated surfaces indicate similar surface energies for  $\gamma$  and  $\alpha$  phases, as has been reported before.<sup>3</sup> For anhydrous surfaces, crossover in stability between  $\gamma$ - and  $\alpha$ -Al<sub>2</sub>O<sub>3</sub> is observed for pure and doped Al<sub>2</sub>O<sub>3</sub>. The crossover in stability of  $\gamma$ -alumina with additives occurs at lower surface areas than for pure Al<sub>2</sub>O<sub>3</sub>, thus reflecting a lesser thermodynamic driving force behind the observed delayed crystallization of both Zr- and Mg-doped samples, though the delays are of different origins.

(19) Lodziana, Z.; Topsoe, N. Y.; Norskov, J. K. *Nature Mater.* **2004**, *3*, 289.

(20) Coster, D. J.; Fripiat, J. J.; Muscas, M.; Auroux, A. *Langmuir* **1995**, *11*, 2615.

(21) Thiel, P. A.; Madey, T. E. *Surf. Sci. Rep.* **1987**, *7*.

(22) Gervasini, A.; Auroux, A. *J. Phys. Chem.* **1993**, *97*, 2628.

(23) Cerofolini, G. F. *Surf. Sci.* **1975**, *51*, 333.

(24) Brunauer, S.; Kanro, D. L.; Weise, C. H. *Can. J. Chem.* **1956**, *34*, 1483.

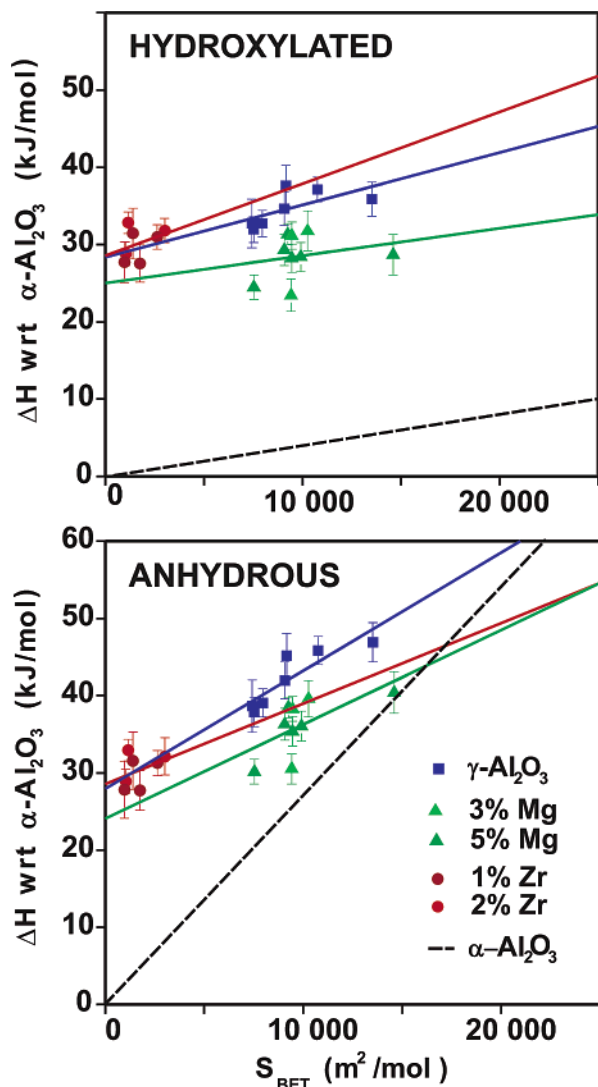


**Figure 4.** Excess enthalpies of pure and doped  $\gamma$ -Al<sub>2</sub>O<sub>3</sub> versus surface area of the samples. Coarse  $\alpha$ -Al<sub>2</sub>O<sub>3</sub>, MgO, and *m*-ZrO<sub>2</sub> are taken as reference states. The intercepts indicate excess enthalpy of  $\gamma$ -Al<sub>2</sub>O<sub>3</sub> compositions with virtual zero surface area; the slope of the lines corresponds to surface enthalpies. The trends for high-surface area  $\alpha$ -Al<sub>2</sub>O<sub>3</sub> are from McHale et al.<sup>3</sup>

**Table 2.** Calorimetrically Derived Surface Enthalpies (J/m<sup>2</sup>)

	hydroxylated ( $\Delta H_{\text{des}} = 0$ )	anhydrous ( $\Delta H_{\text{des}} = -\Delta H_{\text{ads}}$ )
$\alpha$ -Al <sub>2</sub> O <sub>3</sub> <sup>a</sup>	0.4	2.04
$\gamma$ -Al <sub>2</sub> O <sub>3</sub> <sup>b</sup>	0.68	1.53
Mg-doped $\gamma$ -Al <sub>2</sub> O <sub>3</sub> <sup>b</sup>	0.35	1.22
Zr-doped $\gamma$ -Al <sub>2</sub> O <sub>3</sub> <sup>b</sup>	0.93	1.04
<i>t</i> -ZrO <sub>2</sub> <sup>c</sup>	1.02	1.23
Am-ZrO <sub>2</sub> <sup>d</sup>	0.5	
Am-SiO <sub>2</sub> <sup>e</sup>	0.13	0.26

<sup>a</sup> See ref 3. <sup>b</sup> This work. <sup>c</sup> See ref 12. <sup>d</sup> See ref 1. <sup>e</sup> See ref 24.

In the case of Zr, a lower surface energy for the anhydrous phase compared with pure  $\gamma$ -alumina means that at a given surface area,  $\gamma$ -alumina doped with Zr will be less thermodynamically unstable over coarse corundum. Mg does not change the surface energy of  $\gamma$ -alumina significantly, but it decreases its bulk instability (as a hypothetical coarse material) with respect to coarse corundum plus MgO. This can be understood on the basis of the Mg solubility in the  $\gamma$ -Al<sub>2</sub>O<sub>3</sub> spinel structure. Mg fills some of the available cation

vacancies in the spinel structure, forming chemical bonds similar to those found in isomorphous MgAl<sub>2</sub>O<sub>4</sub>. The formation of the solid solution (often formulated as MgAl<sub>2</sub>O<sub>4</sub>-Al<sub>8</sub>O<sub>3</sub>) is, therefore, expected to decrease the bulk instability.

It is interesting to note that the surface enthalpy of Zr-doped  $\gamma$ -alumina is higher than that for pure  $\gamma$ -alumina for the hydroxylated surface but is lower for the anhydrous surfaces. This affects the coarsening behavior of these powders and is consistent with the specific surface area data in Figure 2. The surface areas of Zr-doped  $\gamma$ -alumina powders at temperatures higher than 950 °C are all smaller than that of pure  $\gamma$ -alumina. However, the slopes of the Zr-doped linear fittings are lower than that for pure  $\gamma$ -alumina. Although this looks paradoxical, it reflects the fact that, at lower temperatures, water coverage is expected on the surface of the  $\gamma$ -alumina. This causes Zr-doped alumina to coarsen faster than pure  $\gamma$ -alumina because of the higher surface energies. However, when water desorbs from the surface at temperatures above ~900 °C, coarsening proceeds much more slowly than in pure and Mg-doped  $\gamma$ -Al<sub>2</sub>O<sub>3</sub> (Figure 2).

Considering that the surface energies are derived from small differences of large numbers, the uncertainty calculations for surface energies derived by linear fitting of all data points yield values from  $\pm 0.4$  J/m<sup>2</sup> for pure  $\gamma$ -Al<sub>2</sub>O<sub>3</sub> to  $\pm 1$  J/m<sup>2</sup> for Zr-doped  $\gamma$ -Al<sub>2</sub>O<sub>3</sub>. Though the calorimetric data do not justify nonlinear fitting, one must keep in mind that variation of surface energy with particle size may be more complicated. For instance, in modeling of  $\theta$ -alumina surfaces, the nonlinear variation of surface energies with slab thickness was predicted even if edge effects were neglected.<sup>19</sup> Nevertheless, despite the uncertainties, derived surface energies in the linear fits are acceptable and have been used consistently to study size-dependent phase transformations.<sup>1,3,12</sup> Furthermore, the Zr effect in decreasing the surface energy of  $\gamma$ -Al<sub>2</sub>O<sub>3</sub> is also strongly supported by the adsorption calorimetry data presented in Figure 3.

If Zr doping decreases the surface energy of anhydrous  $\gamma$ -Al<sub>2</sub>O<sub>3</sub>, one may suspect the formation of excess ZrO<sub>2</sub> at the surface as reported for Fe- and Ni-doped SnO<sub>2</sub>.<sup>25,26</sup> For an independent crosscheck, Zr/Al ratios in the samples quenched from 50 °C below the  $\gamma$ - $\alpha$  transformation temperature were measured by X-ray photoelectron spectroscopy. The values obtained for the samples with 1 and 2 mol % Zr doping were  $0.0062 \pm 0.0001$  and  $0.0156 \pm 0.0001$ . This indicates 17 and 27% enrichment in Zr near the surface with respect to the Zr/Al ratios in the bulk measured by electrons microprobe,  $0.0050 \pm 0.0008$  and  $0.0120 \pm 0.0008$ . Both hydroxylated and anhydrous surfaces of Zr-doped alumina have lower average enthalpies than those of tetragonal zirconia.<sup>12</sup>

## Conclusions

The results reported here show the dependence of the energetics on the presence of additives in  $\gamma$ -alumina. These

- (25) Castro, R. H. R.; Hidalgo, P.; Coaquira, J. A. H.; Bettini, J.; Zanchet, D.; Gouvea, D. *Eur. J. Inorg. Chem.* **2005**, *11*, 2134.  
 (26) Hidalgo, P.; Castro, R. H. R.; Coelho, A. C. V.; Gouvea, D. *Chem. Mater.* **2005**, *17*, 4149.

observations not only have implications for theoretical discussions of the influence of dopants on the alumina phase transformation, but can also be proposed as a new tool for controlling phase transformations in ceramic materials. In fact, there is no reason to believe this behavior is restricted to alumina powders, and similar effects may occur for BaTiO<sub>3</sub>, ZrO<sub>2</sub>, and other systems with phase transformations. The modification of surface energy by dopants may also influence other surface-dependent phenomena, such as sin-

tering and grain size control, opening new perspectives on the study and control of these phenomena.

**Acknowledgment.** The work at University of California, Davis, was supported by the U.S. Department of Energy, Grant DE-FG03-01ER15237. Brazilian institutes FAPESP (proc. 96/09604-9, 99/10798-0, 01/10053-7) and CAPES are also acknowledged for financial support.

CM052599D